of inertia of the structures determined by using the MM2 program. The agreement is quite good.

In our force field calculations of molecules other than hydrocarbons, a bond-moment scheme[12] is used in order to calculate dipole moments and point dipoles are used to represent the bond moments. an electrostatic calculation, originally due to Jeans and subsequently modified,[9,15] was employed to estimate electrostatic energies, which must be included in the calculations.

Bond-moment schemes for calculating dipole moments have long been used, and they are in general semiquantitative in their results.[9] One reason for their limited accuracy is that they only allow for the standard moments between atom pairs. The induced moments which result when a sizable dipole is placed into a highly polarizable environment are not taken into account. Our force field dipole–dipole calculations[9,11] are of this sort. In practice such calculations prove to be adequate for predicting structures. For energies and for dipole moments, the results are often only semiquantitative. Nonetheless, this is the scheme used by our molecular mechanics program.

Because of the discrepancy between the dipole moment for the lactone calculated by this method (3.81 D) and that found experimentally (4.71 D), we decided to have a look at a more refined technique for dipole moment calculation. This is a procedure originally due to Eyring,[16] and it is subsequently modified and extended.[17] In the latest version,[18] it permits one to allow completely for the induced moments throughout the molecule. This procedure gives dipole moments in complex polar molecules which are substantially better than one gets by the simple bond-moment scheme. In the present case, the calculated total moment is indeed appreciably improved, although the agreement with experiment is still not very good. The remaining error is believed to result from the fact that ether and ketone components for the original bond moments are used. Thus they did not account for the ester resonance, and the calculated moments are too small. The results are given in Table V.

In summary, the experimental data show that there are two conformers separated in energy by approximately 0.6 kcal/mol with the more stable conformer having a very small (<0.1 D) μ_c component of the dipole moment. The less stable conformer has a much greater value of μ_c. The rotational constants have been determined from the microwave data.

The use of the MM2 program indicates two stable conformers, a half-chair and a boat form. The half-chair form is calculated to be 0.54 kcal/mol more stable than the boat and to have a value of μ_c of the order of 0.01–0.02 D. In addition, the rotational constants for this half-chair conformer are in good agreement with those determined experimentally for the more stable conformer. The values of μ_c predicted for the boat conformer (0.96–1.06 D) are in agreement with the qualitative experimental result on the magnitude of μ_c for the less abundant conformer. The calculated rotational constants for this boat conformer are in agreement with those found experimentally from the microwave spectrum.

(15) J. M. Lehn and G. Ourrison, *Bull. Soc. Chim. Fr.*, 1113 (1963).
(16) R. P. Smith and H. Eyring, *J. Am. Chem. Soc.*, **74**, 229 (1952), and subsequent papers.
(17) N. L. Allinger and M. T. Wuesthoff, *Tetrahedron*, 33, 3 (1977); L. Dosen-Micovic and N. L. Allinger, *ibid.*, **34**, 3385 (1978).
(18) L. Dosen-Micovic, thesis submitted to the University of Belgrade, 1979.

Direct Measurements of Tetraphenylethylene Torsional Motion by Picosecond Spectroscopy

P. F. Barbara, S. D. Rand, and P. M. Rentzepis*

Contribution from Bell Laboratories, Murray Hill, New Jersey 07974. *Received June 9, 1980*

Abstract: We have investigated the *time-* and *wavelength*-resolved fluorescence of tetraphenylethylene (TPE) induced by 355-nm picosecond excitation in several solvents over a range of temperatures and viscosities. Several distinct fluorescence kinetic processes have been identified that are manifested by (i) time-dependent fluorescence spectral shifts, (ii) time-dependent fluorescent spectral-shape changes, and (iii) nonexponential fluorescence decay kinetics. It is found that the relaxation rates of these processes depend strongly on temperature and solvent viscosity. Two of the processes have rates that are greater than 10^{12} s^{-1} at room temperature. The observed fluorescence dynamics of TPE are complex and suggest that several channels are available for excited-state relaxation. We have tentatively assigned the relaxation pathways to radiative and radiationless electronic decay, vibrational relaxation, and two forms of excited-state conformational relaxation. A unified model is proposed for the photochemical dynamics of TPE.

In a photochemical reaction the electronically excited starting material is converted to the stable photoproducts by a number of relaxation processes. The most widely studied and best understood of these are fluorescence and phosphorescence. A considerable effort has also been expended in the study of radiationless vibrational and electronic transitions, which have recently been monitored directly by means of picosecond spectroscopy.[1-3] One of the least studied processes, in contrast, is excited-state conformational relaxation, which is commonly believed to be significant for photochemical reactions in which the starting material and product stereochemistry greatly differ. Examples include cis–trans isomerization[4] and intramolecular cyclization.[5]

(1) P. F. Barbara, L. E. Brus, and P. M. Rentzepis, *Chem. Phys. Lett.* **69**, 447 (1980).
(2) P. F. Barbara, P. M. Rentzepis, and L. E. Brus, *J. Chem. Phys.*, **72**, 6802 (1980).
(3) For examples of picosecond studies of electronic radiationless decays: (a) L. J. Noe, E. O. Degenkolb, and P. M. Rentzepis, *J. Chem. Phys.*, **68**, 4435 (1978); (b) K. G. Spears and M. El-Manguch, *Chem. Phys.*, **24**, 65 (1977); (c) H. B. Lin and M. Topp, *Chem. Phys. Lett.*, **64**, 452 (1979).
(4) (a) G. Fischer, G. Seger, K. A. Muszkat, and E. Fischer, *J. Chem. Soc., Perkin Trans. 2*, 1569 (1975); (b) M. A. El-Bayoumi and F. M. Abdel-Halim, *J. Chem. Phys.*, **48**, 2536 (1968); (c) H. Stegemeyer, *Chem. Ber.*, **72**, 335 (1968); (d) J. Kordas and A. El-Bayoumi, *J. Am. Chem. Soc.*, **96**, 3043 (1974). (e) C. O. DeBoer and R. Y. Schlessinger, *ibid.*, **90**, 803 (1968); J. Salliel, O. C. Zafirious, E. D. Megarity, and A. A. Lamola, *ibid.*, 4759 (1968).
(5) D. Billen, N. Boens, and F. C. De Schrijver, *J. Chem. Res. Synop.*, 79 (1979); F. B. Mallory, J. T. Gordon, and C. S. Wood, *J. Am. Chem. Soc.*, **85**, 828 (1963); **86**, 3094 (1964); E. Fischer and K. A. Muszkat, *J. Chem. Soc. B.*, 662 (1967); E. Fischer, *Fortschr. Chem. Forsch.*, **7**, 605 (1967).

0002-7863/81/1503-2156$01.25/0

Even though excited-state conformational changes are likely to be an influential mechanism of organic photochemistry, the kinetics of such structural changes have not been studied experimentally until recently[6] due to the complexity of the processes and the difficulty of observing the fast kinetics which dominate the conformational dynamics. Published results, to date, have uncovered the coarse features of excited-state conformational changes. Further experimentation, particularly time-resolved spectroscopy, is needed to gain a detailed understanding of this complex and important process.

Lately picosecond fluorescence spectroscopy has been utilized with considerable success for direct measurement of the growth and decay of emission from the various configurational states through which a molecule passes following photon excitation. This method has been particularly successful in the study of ultrafast excited-state proton transfer,[6a,7] vibrational relaxation in large organic molecules in condensed media,[1,2,6a,7] and radiative and radiationless electronic decay.[3b,c,6a] The inherent advantages of time-resolved fluorescence are a large dynamic range, high sensitivity, and a time scale extending from 1 ps to nanoseconds. The capability of measuring subtle changes in the time-dependent fluorescence band shape and intensity allows for the monitoring of variations in the instantaneous molecular geometry and intramolecular energy content.

In this paper we apply picosecond fluorescence spectroscopy to the study of the photochemical dynamics of tetraphenylethylene (TPE) as a function of viscosity and temperature, with particular emphasis on excited-state conformational relaxation. It is commonly believed[4] that this compound, and the related *cis*- and *trans*-stilbenes, exhibit viscosity-dependent conformation dynamics, in their first excited singlet state (S_1), that are primarily characteristic of torsional motion about the ethylenic bond. The scope of this investigation is the observation and assignment of the various torsional decay channels for TPE and the identification of the other pathways through which the excitation energy is dissipated, such as electronic and vibrational relaxation.

Experimental Section

The experimental data presented here were obtained with two experimental systems: (1) a picosecond emission spectrometer which has been described in detail elsewhere[1] and (2) a nontime resolved emission spectrometer. The major components of the picosecond system are a Nd^{3+} mode-locked silicate glass laser emitting 6-ps 1060-nm pulses, which are used to generate third harmonic 355-nm excitation pulses, and an Imacon 675 Photocon II streak camera with ≤5-ps resolution. The optical streak image is digitized by a PAR 1205A multichannel analyzer and processed by a Nova computer. The spectral resolution was achieved by means of interference filters.

The picosecond data shown here represent a time average of the fluorescence induced by 10–20 laser pulses. Typically, the experimental data for intensity vs. time are fitted by a nonlinear least-squares convolution procedure employing an assumed kinetic model and the actual time dependence of the laser pulse.[1] This is illustrated by the computer generated curves shown in some figures. The kinetic model assumes that the population of the fluorescing state is fed from the initially excited state by a first-order reaction with inverse rate constant, τ_r, and consumed by a first-order reaction with fluorescence lifetime, τ_f. We have previously demonstrated[1] that our apparatus is capable of resolving $\tau_r \leq 5$ ps and τ_f in the range 10–5000 ps with ~10% accuracy.

The total fluorescence spectra presented in Figure 1 were not time resolved, rather they were recorded by a vidicon attached to a 0.32 m, 3205 PAR spectrometer and a 1205A PAR optical multichannel analyzer. The advantage of this arrangement was that it allowed the recording of spectra in the identical optical arrangement and excitation conditions as the picosecond time-resolved experiments.

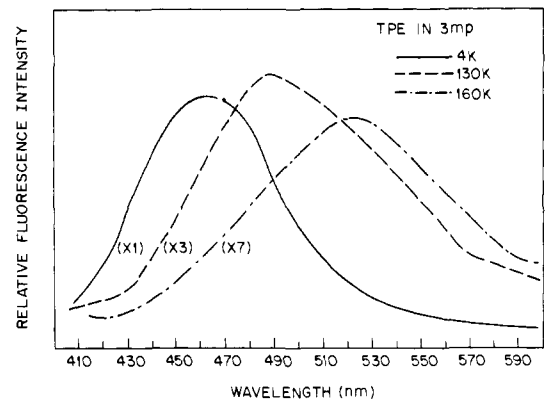

Figure 1. Fluorescence spectra of TPE in 3MP glass after excitation with a single 355-nm picosecond pulse. The spectra were recorded at 4 (—), 130 (– – –), and 160 K (– · –); none of these spectra were time resolved.

The sample cell and cryogenic system have been described previously.[1,7] TPE was purchased from Aldrich Chemical and recrystalized from toluene. The fuorescence spectra of the samples were very similar to those previously reported.[4a,c] Under time-resolved conditions, however, a weak long-lived impurity emission was observed. The latter was decreased by a factor of 50 by recrystallization from 3-methylpentane, 3MP. The effect of this impurity emission on the TPE spectra and the determined kinetics was negligible. Spectroscopic or reagent grade solvents were used to make the sample solutions which were typically $<10^{-4}$ M in TPE.

Results and Discussion

The experimental data fall into three categories. The first type displays the complete fluorescence spectrum in the standard form intensity vs. wavelength, without any time-dependent information (Figure 1). In the second type we show time-resolved fluorescence within certain 10-nm wavelength regions. The third type of data exhibits the decay kinetics of the complete fluorescence spectrum and is used in calculating fluorescence lifetimes, τ_f. In general we observed that the total fluorescence decays by a dominant first-order process that accounts for approximately 80% of the signal decrease and some slower multiexponential channels, which well be discussed in some detail below. In the discussion of the results, reference to fluorescence lifetime, τ_f, corresponds to only the dominant decay,[9] while the minor ones will be explicitly designated.

Fluorescence Spectra as a Function of Temperature. The fluorescence properties of TPE were found to be very sensitive to temperature and the physical properties of the solvent. TPE excited at 355 nm in 3MP (glass or liquid) exhibits the fluorescence spectra displayed in Figure 1. In agreement with previous observations[4a] in similar solvents,[4a,c] e.g., 2MP, MCH-IP, we find that the fluorescence exhibits a substantial bathochromic shift as a function of temperature. Three distinct regions were identified: (1) Between 4 and 90 K the fluorescence with a maximum at ~460 nm is practically temperature independent. (2) A large spectral shift is observed as a function of temperature between 95 and 125 K. (3) The fluorescence band shape with a maximum at 525 nm is temperature independent above 160 K. The fluorescence intensity was also found to be strongly temperature dependent decreasing by a factor of ~7 from 4–160 K (Figure 1) and by several orders of magnitude over the range 4–293 K.

Fluorescence Decay Kinetics: Torsionally Induced Electronic Radiationless Decay. It is well-known[4] for TPE and the other arylethylenes that torsional motion in the excited state is capable of inducing radiationless electronic decay, $S_1 \rightarrow S_0$. It has been suggested,[4] on the basis of substantial increases in the fluorescence quantum yield in highly viscous solvents and frozen glass, that

(6) (a) P. F. Barbara, L. E. Brus, and P. M. Rentzepis, *J. Am. Chem. Soc.*, **102**, 5631 (1980); (b) F. Heisel, J. A. Miehl and B. Sipp, *Chem. Phys. Lett.*, **61**, 115 (1979); (c) J. R. Taylor, M. C. Adams, and W. Sibbett, *Appl. Phys. Lett.*, **35**, 590 (1979); (d) B. I. Greene, R. M. Hochstrasser, and R. B. Weisman, *Chem. Phys. Lett.*, **62**, 427 (1979); (e) B. I. Greene, R. M. Hochstrasser, and R. B. Weisman, *J. Chem. Phys.*, *71*, 544 (1979); (f) H. H. Klingenberg, E. Lippert, and W. Rapp, *Chem. Phys. Lett.*, **18**, 417 (1973); (g) W. Rapp, *ibid.*, **27**, 187 (1974).

(7) P. F. Barbara, L. E. Brus, and P. M. Rentzepis, *J. Am. Chem. Soc.*, **102**, 2786 (1980).

(8) K. K. Smith and K. J. Kaufman, *J. Phys. Chem.*, **82**, 2286 (1978); W. M. Helherington III, R. H. Michaels, and K. B. Eisenthal, *Chem. Phys. Lett.*, **66**, 230 (1979).

(9) In cases where the fluorescence decay showed a dominant exponential decay with additional minor (<20%) components, the dominant lifetime, τ_f, was determined from a computer fit of the kinetics of the initial 60% decrease in signal intensity.

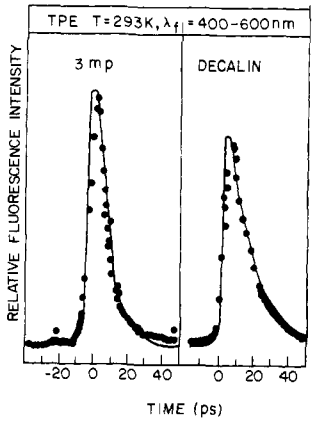

Figure 2. Fluorescence decay of TPE as a function of viscosity: left side 3MP, η = 0.31 cP, τ = 6 ps; right side decalin, η = 2.1 cP, τ = 15 ps.

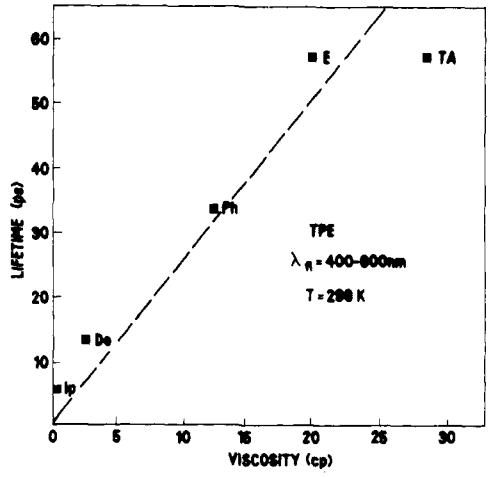

Figure 3. Lifetime of TPE fluorescence as a function of viscosity. IP = isopentane, De = decalin, Ph = phenol, E = ethylene glycol, TA = triacetin.

the torsional motion responsible for inducing radiationless decay is hindered by the viscous drag of the solvent. In the simplest model rotation about the ethylenic bond in S_1 is the most significant process. It is enhanced by periplanar repulsion from the phenyl rings and allowed by the weakening of the ethylenic bond in S_1 (a π–π^* state). Experimental evidence[4a] suggests that only S_0 and S_1 are populated during the photochemical reaction of TPE in hydrocarbon solutions.

Support of this reasoning is provided by the observed dependence of the fluorescence quantum yield, Φ, on molecular structure. The majority of arylethylenes[4a-d] exhibit very little fluorescence, $\Phi \sim 0.001$, at room temperature. Exceptions are found in those molecules that are incapable of torsion about their ethylene bond because of rigid structures.[4e] These rigid molecules exhibit $\Phi \sim 1$. Thus ethylenic bond torsion in S_1 is apparently required for radiationless decay.

The lifetime of the fluorescence for TPE is shown in Figures 2 and 3 to increase from 6 ps in low viscosity room temperature 3MP to 15 ps in decalin and to almost 60 ps in ethylene glycol. The lifetime increases to 600 ps in highly viscous glycerol. In agreement with previous proposals,[4a,c] the excited-state decay rate decreases with increasing solvent viscosity. We have plotted in Figure 4 the log of the inverse lifetime (rate constant) vs. inverse temperature. This is essentially an Arrhenius plot for the radiationless decay. The lifetimes employed in this figure have been corrected for radiative decay. As expected from previous quantum yield measurements,[4] we observe a strong decrease in the radiationless decay rate at low temperature.

These observations are consistent with the previously published nontime resolved[4a,c] results and nanosecond fluorescence[6f] measurements and are supportive of the traditional explanation for the temperature dependence of the TPE photodynamics. In this

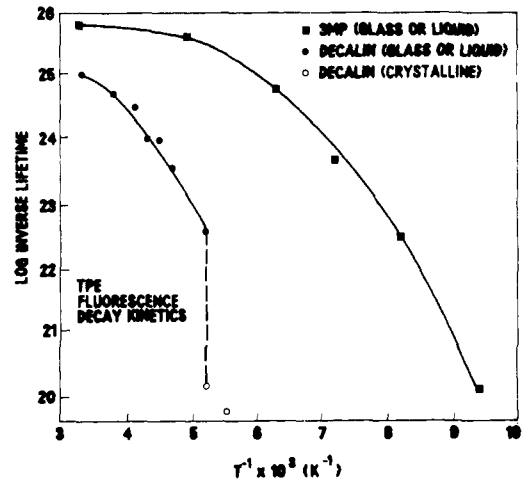

Figure 4. Arrhenius plot, ln k vs. $1/T$, for TPE dissolved in 3MP (■) decalin glass (●) and decalin crystalline (○), where $k = (\tau_T^{-1} - \tau_{4K}^{-1})$, and τ_{4K} = 5.5 ns.

model[4] the temperature dependence of the electronic radiationless decay rate is not due to an intramolecular activation energy but rather is derived from a temperature-dependent solvent viscosity which controls the rate of torsionally induced electronic radiationless decay. In other words, as the solvent viscosity increases at lower temperatures, the torsional motion is hindered, and consequently, the radiationless decay rate decreases.

This is supported by the observation that the decay rate is almost 3 orders of magnitude slower in crystalline decalin than in the less rigid decalin glass, both at 192 K (see Figure 4). This experiment is accomplished by recording the fluorescence kinetics prior and subsequent to solvent crystallization which occurs spontaneously[10] in decalin at 192 K. The observed curvature in the Arrhenius plots of Figure 4 for the radiationless decay also suggests that the dominant relaxation mechanism is not a simple thermally activated process, which would exhibit a linear Arrhenius plot. Interestingly, the most curvature for the decay in 3MP occurs around the glass forming temperture of the solvent[11] where viscosity and solvent structure are changing drastically. Another indication that temperature dependent viscosity controls the observed temperature dependence is the large change in the rate at temperatures above 100 K when decalin is substituted for the less viscous 3MP, which otherwise has similar properties, e.g., polarizability and dielectric constant.

Spectral Band-Shape Changes: Intermediate Temperatures (90–160 K). As we mentioned previously, the fluorescence spectra of TPE undergoes an abrupt bathochromic shift as the solvent viscosity decreases by increasing the temperature or substituting a less viscous solvent. It has been argued[4c] that this red shift results from an extensive torsional arrangement in S_1 whose rate is strongly diminished in highly viscous media. Presumably, the fluorescence spectrum at low temperatures, <90 K, is characteristic of the initially excited, unrearranged conformation(s) of S_1, while at higher temperatures, the fluorescence is partly due to the rearranged conformation(s) of S_1.

This model predicts that the time-dependent fluorescence spectrum should shift toward longer wavelengths during the lifetime of the excited state. In particular, the short-wavelength region (ca. 425 nm) of the total spectrum should appear with an instantaneous rise time, characteristic of the unrearranged geometry, *and* decay with a lifetime, τ_f, that, in part, represents the time scale for excited-state rearrangement. The long wavelength region of the spectrum (ca. 550 nm), characteristic of the rear-

(10) If the decalin solution is cooled rapidly (<4 min) from 298 to 192 K, crystal growth is visible on the walls of the sample cell in ~15 min. The solution appears to be entirely crystalline in ~25 min.

(11) I. Norman and G. Porter, *Proc. R. Soc. London, Ser. A*, **230**, 399 (1955).

(12) P. Borrell and H. H. Greenwood, *Proc. R. Soc. London, Ser. A*, **298**, 453 (1967).

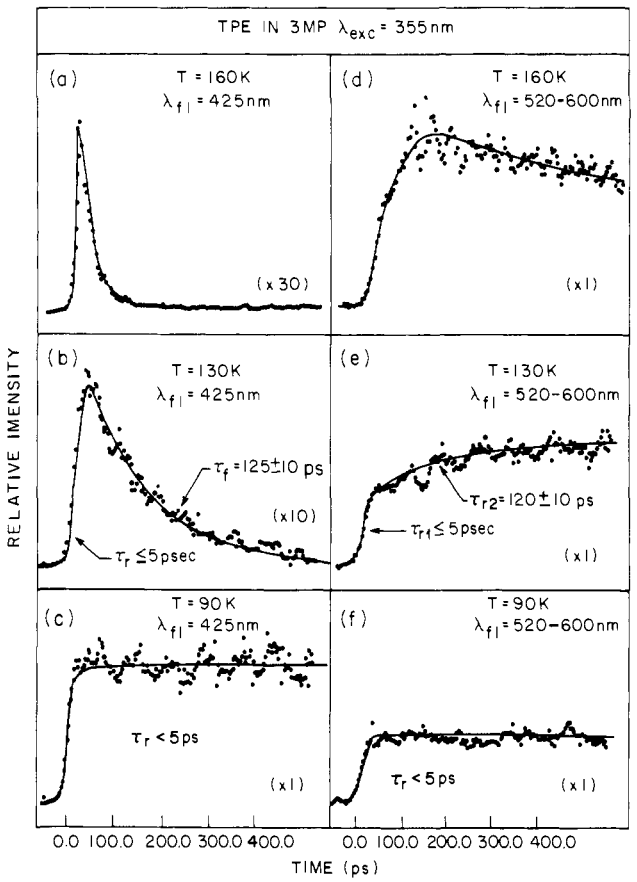

Figure 5. Formation and decay kinetics of the TPE fluorescence as a function of temperature (viscosity) and emission wavelength. Left side figures show the kinetics of the high energy region of the emission spectrum at (a) T = 160 K, (b) T = 130 K, (c) T = 90 K. The kinetics of the right hand figures were measured between 520–600 nm at (d) T = 160 K, (e) T = 130 K, and (f) T = 90 K. Solid lines represent computer fits.

ranged conformation(s) of S_1, should exhibit a *rise time equal to the lifetime of the short wavelength fluorescence.* Fortunately, our experimental apparatus is well suited to test the above predictions with its ability to detect short lifetimes and small spectral shifts.

Our results for both time *and* wavelength-resolved fluorescence are displayed in Figure 5. The left three panels show the time dependence in the short wavelength portion of the fluorescence spectrum, while the right panels display the time dependence in the intermediate to long wavelength portions. Due to the weak red response of our streak camera photocathode, it was not possible to record the time dependence of the extreme (>600 nm) long wavelength fluorescence region.

At 90 K we observe identical kinetics in the short and long wavelength regions of the spectrum, i.e., a ≤4 ps rise time and a ~5-ns decay lifetime, see Figure 5c,f. Apparently at 90 K the fluorescence band does not shift on the 4–5000-ps time scale. The kinetics at 130 K are dramatically different from the low temperature results. In the 425-nm region, a pulse limited risetime is observed with a 125 ± 10-ps decay time (see Figure 5b). The long wavelength fluorescence from 520 to 600 nm, in contrast, exhibits a decay time of ~5 ns and *two* rise times (see Figure 5e). One of these is pulse limited (<4 ps) and is probably due to the long wavelength edge of fluorescence from the same species that is responsible for the 524 nm kinetics. The second rise time is 120 ± 10 ps which is *equal*, within experimental error, to the *decay* time of the 425-nm fluorescence. Presumably, the 160–165-ps value represents *the time scale for interconversion of the short to long wavelength fluorescence.* At 160 K, the interconversion time scale is faster, ~15 ps.

The kinetics displayed in Figure 5 are highly supportive of the kinetic bathochromic shift mode. We observe that the fluorescence

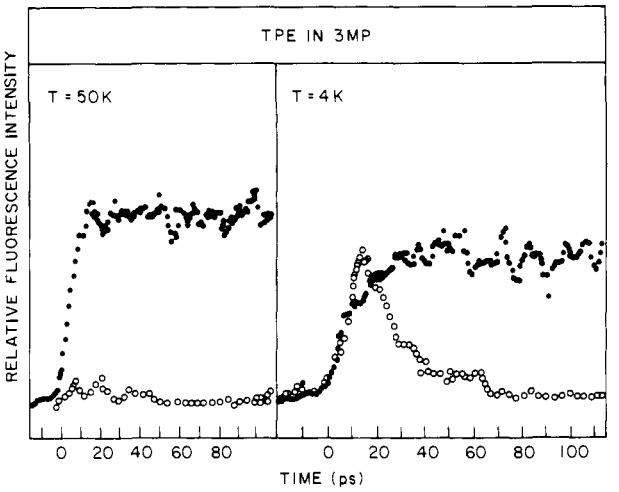

Figure 6. Low temperature kinetics of TPE fluorescence in 3MP, at 380 nm and 425 nm. Left figure T = 50 K; right figure T = 4 K (open circles, ○, 380 nm; solid circles, ●, 420 – 600 nm).

band shifts in time, and that this fluorescence shift is strongly temperature (viscosity) dependent. An analysis of the nanosecond dynamics of the fluorescence at 90 K and below indicates that no significant bathochromic shift occurs during the excited-state lifetime at low temperatures.

With respect to the radiationless decay process, we observe that the long wavelength fluorescence *decays* at a much slower rate than the interconversion of short to long wavelength fluorescence. This suggests strongly that *the rearrangement responsible for the bathochromic shift is independent of the rearrangement responsible for inducing radiationless decay.*

Spectral Band-Shape Changes: Low Temperature (4–50 K). Recently, we observed ultrafast fluorescence band-shape changes at low temperature (4–50 K) for several large molecules[2,6a,7] which we interpreted as vibrational relaxation after initial Franck–Condon excitation to high vibrational levels of the first excited electronic state. We were able to observe for tetracene[2] at 4 K both "hot" fluorescence, which was produced promptly and decayed in approximately 40 ps, and relaxed fluorescence which exhibited a rise time delay. Above 80 K the relaxation became faster than 4 ps, the instrumental resolution.

TPE, as compared to tetracene, has a more complex excited-state relaxation scheme that involves at least two types of torsional processes (see above). It is interesting to examine whether it is possible to identify small amplitude vibrational relaxation in TPE and to distinguish between the vibrational and torsional processes.

The key to separating the vibrational and torsional relaxation is found in the temperature dependence of the latter processes. At temperature below 90 K, as shown above, both the bathochromic shift process and the torsionally induced radiationless decay are negligibly slow due to the rigidity of the environment. It is at these low temperatures that we examine whether TPE exhibits ultrafast fluorescence band-shape changes that might be interpreted as vibrational relaxation.

TPE is excited in the present experiments at 355 nm, which is close to the maximum of the broad diffuse electronic absorption. This is about 4000 cm^{-1} more energy than the high energy edge (425 nm) of the 4-K fluorescence. It is very difficult to estimate the exact amount of excess vibrational energy imparted to S_1 by excitation from such structureless spectra. It seems reasonable, however, to expect that as much as 4000 cm^{-1} may be in excess.

Our experimental investigation of the time-resolved fluorescence of TPE in the 4–50 K range (see Figure 6) reveals the importance of vibrational relaxation and initial excess vibrational energy content. We observe directly the presence of unrelaxed hot fluorescence at 380 nm with a rise time of ≤4 ps and a decay time of 15 ± 5 ps. We have also found that the kinetics are identical at every part of the 420–600-nm region. The kinetics at 425 nm are shown in Figure 6 for 4 and 50 K. It is evident that these results are remarkably similar to those observed for tetracene.[2]

Table I. Kinetic Processes for TPE Relaxation

assignment	proposed pathway (see Scheme II)	manifestation	T, K	τ^{-1}	figure
vibrational relaxation	$S_{1A}^* \rightarrow S_{1A}$	spectral shift (time dependent)	4	$\sim 10^{11}$	6
			>50	$>10^{12}$	6
torsional rearrangement	$S_{1A} \rightarrow S_{1B}$	spectral shift (time dependent)	4–90	$<10^9$	5
			110–160	10^9–10^{10}	5
			170–293	10^{10}–10^{12}	
torsionally induced electronic radiationless decay (major component)	$S_{1B} \rightarrow S_{1C} \rightarrow S_{0C}$	fluorescence decay kinetics (major component)	4–130	$<10^8$	2, 3, 4
			140–293	10^9–10^{10}	2, 3, 4
torsionally induced electronic radiationless decay (minor component)	$S_{1B} \rightarrow S_{1B'} \rightarrow S_{1C} \rightarrow S_{0C}$ or $S_{1B} \rightarrow S_{1C} \rightarrow S_{0C}$ $\rightarrow S_{1C'} \rightarrow S_{0C'}$	fluorescence decay kinetics (minor component)	4–130	$<10^8$	7, 8
			140–293	10^8–10^{10}	7, 8

This fluorescence at 4 K exhibits two risetimes: (1) an instantaneous ~4-ps component and (2) a ~15-ps component. An explanation is that the initial fluorescence originates from the hot vibrational energy distribution, while the fluorescence component with a 15-ps risetime is the relaxed fluorescence. At temperatures above 50 K the rise time for both components are <4 ps, in analogy to the behavior of other polyatomics.[1,2,6a,7]

The similarity of the low temperature ultrafast fluorescence dynamics of TPE to other polyatomics suggests that vibrational relaxation on ~10-ps time scale may be a general phenomenon for such molecules in the condensed phase at low temperature. In the present case, it is especially significant that it has been possible *to differentiate between vibrational energy relaxation and torsional motions by selectively quenching* ($\tau > 10^{-9}$ *s*) *the torsional processes in rigid, low temperature environments.* Such a distinction by temperature should be a more general phenomenon applicable to many molecular systems.

Multiexponential Decay Kinetics. The fluorescence decay kinetics of TPE at certain temperatures are characterized by more than one first-order (exponential) component. A particularly useful way to demonstrate this is a plot of the log of the fluorescence intensity vs. a reduced time variable, t/τ_1, where t is time and τ_1 is the lifetime of the predominant decay component at each temperature (see Figures 7 and 8). This method for plotting stresses the importance of the different decay components as the temperature is varied. For instance, if the experimental decay were singly exponential at all temperatures, Figures 7 and 8 should be a superposition of straight lines. In contrast, if the experimental decays were multiexponential, but with the same proportion of different components at each temperature, Figures 7 and 8 would be a superposition of identical curved lines.

For TPE we observe a more complex behavior. The shape of the semilog curves indicate that each kinetic component of the fluorescence decay has a different temperature dependence. Three features in the kinetics can be identified. First, in the range of temperatures displayed, the decay kinetics in Figures 7 and 8 are always nonsingly exponential. Second, the relative amounts of the primary and secondary decay components are not dramatically effected by temperature, as judged by the observation that the position where the semilog plots deviate from a straight line is not strongly affected by temperature. Third, the rate of the dominant decay component relative to minor process(es) increases mildly with temperature, as manifested by the temperature dependence of the ratio of initial slope to final slope.

These observations indicate that the radiationless decay mechanism for TPE involves a single dominant component and at least one additional component. We have not been able to determine whether the separate kinetic components are due to successively formed intermediates or intermediates formed by parallel relaxation channels. A further discussion of these results is presented in the next section.

Proposed Kinetic Model. The previous section described the observation and measurement of at least four distinct kinetic processes in the excited-state relaxation of TPE (see Table I). At any single temperature the ratio of rates of the different pathways covers several orders of magnitude. In review, the processes

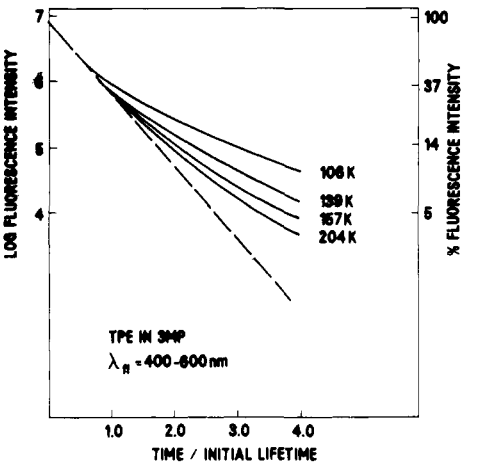

Figure 7. Plot of log fluorescence intensity and percent fluorescence intensity as a function of time divided by initial lifetime of TPE in 3MP at various temperatures. The dotted line is the extrapolated exponential behavior observed during the initial period of decay.

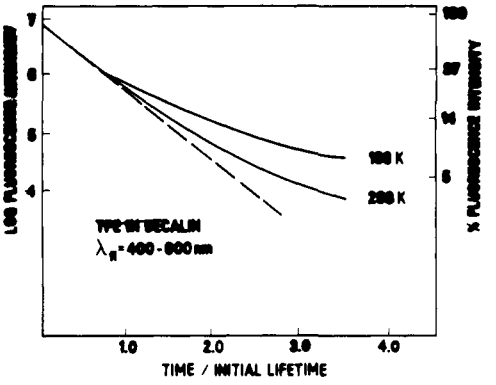

Figure 8. Plot of log fluroescence intensity vs. time divided by the initial lifetime for TPE in decalin between 400–600 nm at 193 and 293 K. The dotted line corresponds to extrapolated exponential behavior observed during the first part of the fluorescence decay.

involved with molecular torsions are slowed significantly in low temperature rigid glass matrices where vibrational relaxation and fluorescence (radiative decay) become the sole relaxation mechanisms. The former, of course, removes localized excess vibrational energy in the excited state, while the latter depletes the electronic excited-state population. At higher temperatures the molecule is apparently capable of rearranging, a process which produces a large kinetic bathochromic shift in the fluorescence spectrum, but does not necessarily induce radiationless decay. At even higher temperatures, however, at least two separate pathways exist for electronic radiationless decay that, judged from the viscosity dependence, involve torsional rearrangements.

In an attempt to construct a unified scheme which incorporates each relaxation mechanism, we have made certain assumptions.

Scheme I

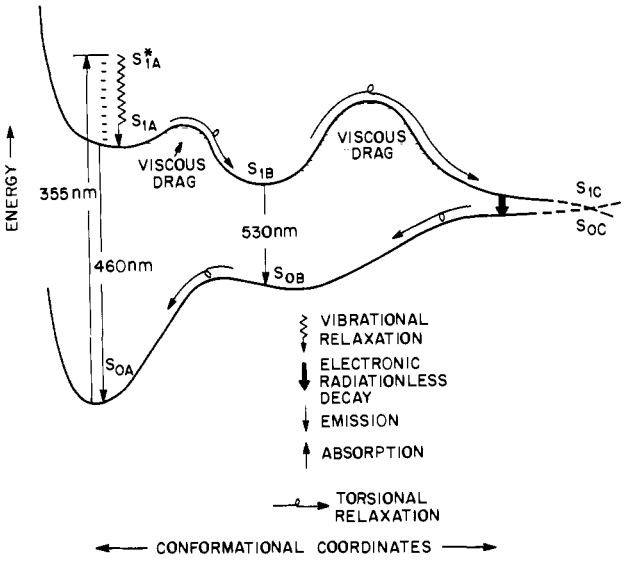

Scheme II

$S_{0A} \xrightarrow{h\nu} S_{1A}^*$	electronic excitation
$S_{1A}^* \xrightarrow{k_{VR}} S_{1A}$	vibrational relaxation
$S_{1A} \xrightarrow{k_r} S_{0A}$	fluorescence
$S_{1A} \xrightarrow{k_{AB}} S_{1B}$	torsional rearrangement
$S_{1B} \xrightarrow{k_{BC}} S_{1C}$	torsional rearrangement followed by rapid electronic radiationless decay
$S_{1C} \xrightarrow{k_{CC}} S_{0C}$	

The simplest is that each of the faster relaxation processes converts the previous kinetically distinct species to the following species in the order of decreasing rates. The temperature dependence of the various mechanisms certainly suggest this should be the case.

Such a kinetic model is represented schematically by Scheme I and outlined by the equations in Scheme II, where the symbol S_{ij} stands for the ith (0,1) excited singlet with jth (A, B, C, D) geometry (conformation). The superscript asterisk indicates excess vibrational energy. The minor component(s) for fluorescence decay (see above) have been ignored in this model but will be discussed below.

Triplet electronic states have not been incorporated in Scheme I because experimental evidence indicates that intersystem crossing is negligible in the photodynamics of TPE.[4a]

Scheme II explains the fluorescence of TPE over the range of temperature and viscosity studies. At low temperature and viscosity, k_{AB} is so slow compared to radiative decay that the fluorescence is characteristic of the A geometry. At higher temperatures (lower viscosities) k_{AB} increases, the spectrum shift toward the red, and the fluorescence is due predominantly to the B geometry. Finally, at even higher temperatures and lower viscosities k_{BC} becomes significant, and S_{1B} rearranges to S_{1C} which is converted rapidly to S_{0C} by nonradiative electronic relaxation. This latter process, of course, shortens the fluorescence lifetime and decreases the fluorescence quantum yield.

Assuming the kinetic validity of Scheme I, the question arises as to the physical significance of the different processes. As mentioned above we have assigned the 4–50-K fluorescence dynamics to vibrational relaxation based on analogy to the spectral characteristic and dynamics of the low temperature fluorescence of a variety of other "rigid" and "flexible" molecules.[1,2,6a,7] In the case of rigid molecules, especially tetracene where the fluorescence spectrum has been analyzed, the assignment of the hot fluorescence was unequivocal.[2] For TPE the assignment relies on the assumption that the rigid, low temperature environment constrains TPE to the S_{1A} conformation. This seems to be supported by our measurements of the rates of the different manifestations of torsional dynamics.

The rearrangement processes that are manifested by the time-dependent bathochromic shift and radiationless decay are controlled to a large extent by solvent viscosity rather than an intramolecular activation energy. This is supported by our kinetic measurements, nanosecond determinations,[6f] and nontime resolved data.[4c] The conformational changes most likely to be sensitive to solvent viscosity are bond torsions which produce large molecular motion.[4,6] Previous studies have tended to stress the importance of motion about the ethylenic bond, θ, based on the qualitative reasoning that the ethylenic bond becomes an essential single bond in the π–π^* state. More sophisticated calculations for arylethylenes, indeed, support large θ replacements.[4a] Motion about the bonds joining the phenyl rings to the ethylene moiety, ϕ, has received less attention, even though calculations suggest that ϕ displacement in S_i may be substantial[4a] in at least the stilbene case.

Our data offer some insight into the question of ϕ and θ motion for TPE if it is assumed that the torsional motion of TPE in S_1 is dependent on viscosity and the extent of molecular deformation but not strongly dependent on a intramolecular torsional potential.[6g] While our data show that intramolecular activation barriers are insignificant, a more careful study of the viscosity dependence of the kinetics is required to determine whether an intramolecular torsional potential is "driving" the rearrangements.[6g]

The different sensitivity on viscosity for the $S_{1A} \rightarrow S_{1B}$ and $S_{1B} \rightarrow S_{1C}$ processes indicates qualitatively that the extent and mode of molecular motion is different for the two rearrangements. In other words, if the two rearrangement processes involved to the same extent ϕ and θ motion, a similar viscosity dependence should be observed. Thus a tentative interpretation would be that ϕ and θ motion are both significant and differ in their importance for the time-dependent bathochromic shift and radiationless decay processes.

Scheme I does not include the minor kinetic component(s) for radiationless decay. As indicated above, we have not been able to identify whether the two or more decay components are due to parallel channels for rearrangement of S_1 or whether successive intermediates are pertinent. Without further information we suggest two elaborations of Scheme I that incorporate the minor decay pathway. The first assumes that S_{1B} is converted first to a weakly fluorescing intermediate $S_{1B'}$, which is converted to S_{1C} by the following route:

$$S_{1B} \rightarrow S_{1B'} \rightarrow S_{1C} \rightarrow S_{0C}$$

The other possibility is that two conformational channels are responsible for the disappearance of S_{1B} according to the following scheme:

$$S_{1B} \rightarrow S_{1C} \rightarrow S_{0C}$$

$$S_{1B} \rightarrow S_{1C'} \rightarrow S_{0C'}$$

where the primes designates alternative conformational states.

Conclusions and Summary

We have investigated the time- and wavelength-resolved fluorescence of TPE induced by 355-nm picosecond excitation in several solvents, temperatures, and viscosities. At least four distinct fluorescence kinetic processes have been identified that are manifested by (i) time-dependent fluorescence spectral shifts, (ii) time-dependent fluorescent spectral-shape changes, and (iii) nonexponential fluorescence decay kinetics. It is found that the relaxation rates of these processes may vary by as much as several orders of magnitude, given a specific choice of solvent and temperature. The individual rates, furthermore, are strongly temperature dependent and at least two of the processes have rates that are greater than 10^{12} s^{-1} at room temperature.

The fluorescence behavior of TPE points toward a mechanism for photochemical and photophysical relaxations that is more detailed than most of the prevailing approaches in organic pho-

tochemistry.[13] It is likely, however, that TPE is not an extraordinary case but rather a general one. We expect that investigations similar to the present, when applied to other molecules, will lead to analogous results and complexity. Indeed, time-resolved fluorescence studies[6b,c,f] of other photochemical systems, over smaller temperature ranges without wavelength resolutions, already indicate that the fluorescence kinetics should be expected to be complex in many cases.

The question, of course, arises as to the physical significance of the different manifestations of excited-state relaxation. The following mechanisms for relaxation are proposed based on our experimental results: (1) small amplitude vibrational relaxation as indicated by picosecond hot fluorescence at low temperature; (2) conformational relaxation as indicated by viscosity controlled time-dependent bathochromic shifts in the spectrum; (3) conformational relaxation inducing electronic radiationless decay from $S_1 \rightarrow S_0$ as indicated by viscosity-dependent lifetimes; and (4) radiative decay of S_1.

We are presently examining the presence of these relaxation processes in the photochemistry of other molecules, including *cis*- and *trans*-stilbenes. It is our goal to apply the methods employed in this paper to gain a detailed understanding of the mechanism responsible for cis-trans isomerization and excited-state torsional motion in general. Potentially, these techniques could lead to a much higher level of specificity and completeness in the understanding of mechanistic photochemistry.

(13) Complexity of this sort, however, has been suggested on theoretical grounds, e.g., J. Michl., *J. Mol. Photochem.*, **4**, 243 (1972); H. E. Zimmerman and M. G. Steinmetz, J. *Chem. Soc., Chem. Commun.* 230 (1978).

Vibrational Studies of (Tetraphenylporphyrinato)cobalt(II) and Its Adducts with CO, NO, and O_2 in Gas Matrices

Muneteru Kozuka* and Kazuo Nakamoto

Contribution from the Todd Wehr Chemistry Building, Marquette University, Milwaukee, Wisconsin 53233. *Received July 31, 1980*

Abstract: The adducts of (tetraphenylporphyrinato)cobalt(II) (Co(TPP)) with axial ligands such as CO, ^{13}CO, NO, $^{16}O_2$, $^{16}O^{18}O$, and $^{18}O_2$ have been studied in Ar and/or Kr matrices with the use of infrared spectroscopy. Formation of the following adducts and their axial ligand frequencies (cm^{-1}) have been confirmed: Co(TPP)$(CO)_2$, 2077 Kr, 2078 Ar; Co(TPP)(CO), 2073 Kr; Co(TPP)$(^{13}CO)_2$, 2032 Ar; Co(TPP)(NO), 1690 Kr, 1693 Ar; Co(TPP)$(^{16}O_2)$, 1278 Ar, 1272 Kr; Co(TPP)$(^{16}O^{18}O)$, 1252 and 1241 Ar; Co(TPP)$(^{18}O_2)$, 1209 Ar, 1207 Kr. The O_2 stretching frequency of Co(TPP)(O_2) is the highest among those of molecular oxygen adducts of Co(II) and Fe(II) chelates known thus far. The doublet band observed for the O_2 stretching vibration of its $^{16}O^{18}O$ adduct definitely indicates the asymmetric end-on coordination of molecular oxygen. Resonance Raman spectra of Co(TPP) in matrices of respective ligands have shown the presence of the Co–ligand vibrations at 231, 237, and 345 cm^{-1} for Co(TPP)$(^{13}CO)_2$, Co(TPP)$(CO)_2$, and Co(TPP)(O_2), respectively. Formation of the mixed-ligand adducts such as Co(TPP)(CO)(NO) and Co(TPP)(CO)(O_2) has been confirmed, and the effect of trans-ligand interactions discussed.

Cobalt(II) chelates of porphyrins and Schiff base ligands have been the subject of extensive investigations in the past decade due to their ability to form molecular oxygen adducts. The techniques used to study these adducts include X-ray analysis, MO treatments, and electronic, ESR, and vibrational spectroscopy together with kinetic and thermodynamic measurements.[1] Very few reports are available, however, on the reactions of Co(II) chelates with other ligands such as CO and NO. As to Co(TPP) (TPP = tetraphenylporphyrinato anion), Wayland et al.[2] discussed the electronic structures and bonding of its adducts with CO, NO, O_2, $P(OCH_3)_3$ and nitrogen donors based on their ESR and electronic spectra in toluene solution. However, no detailed vibrational studies have been made on these adducts. This paper reports the infrared (IR) and resonance Raman (RR) spectra of Co(TPP) complexed with CO, ^{13}CO, NO, $^{16}O_2$, $^{16}O^{18}O$, and $^{18}O_2$ in low-temperature gas matrices. The matrix-isolation technique is ideal for such a study since most of these adducts are stable only at very low temperatures. It should be noted that previous vibrational studies have been concentrated on molecular oxygen adducts with base ligands at the sixth coordination site. In this respect, our study is unique since Co(TPP)O_2 formed in inert-gas matrices can provide information about the O_2 and Co–O_2 bonds in the absence of a base ligand. Finally, matrix-isolation spectra are free from interference by solvent bands which often hinders the analysis of vibrational spectra obtained in solutions.

* To whom correspondence should be addressed at the Chemical Research Institute of Nonaqueous Solutions, Tokoku University, Sendai 980, Japan.

Experimental Section

Co(TPP) was prepared by the literature method[3] and purified by chromatography on an alumina column and recrystallization from $CHCl_3$–CH_3OH. The gases, O_2 (99.99%, Matheson), $^{18}O_2$ (92% Monsanto Research), CO (99.99%, Matheson), ^{13}CO (90.5%, Merck), NO (99.0%, Matheson), Ar (99.9995%, Matheson), and Kr (99.995%, Airco) were used without further purification. The $^{16}O^{18}O$ gas was prepared by electrical discharge of a mixture of $^{16}O_2$ and $^{18}O_2$, and its mixing ratio was determined by the relative intensities of Raman bands of each species in a mixture which was deposited on a copper cold-tip at ~15 K.[4]

Co(TPP) was vaporized from a Knudsen cell at ~430 K, and codeposited with respective gases on a CsI plate which was cooled to ~15 K by a CTI Model 21 closed-cycle helium refrigerator. A detailed design of the cell is described elsewhere.[5] IR spectra were measured on a Beckman IR-12 infrared spectrophotometer. High-resolution spectra were obtained with use of a 10-cm^{-1}/in. chart expansion, 0.8 cm^{-1}/min. chart speed, and a manual slit program. Rotation–vibration bands of standard molecules were used to calibrate the frequency reading. The miniature oven technique[4] was employed to measure the RR spectra of Co(TPP) in CO, ^{13}CO, NO, and O_2 matrices. The spectra were recorded on a Spex Model 1401 double monochromator. Detection was made with

(1) R. D. Jones, D. A. Summerville, and F. Basolo, *Chem. Rev.*, **79**, 139 (1979), and references therein.
(2) B. B. Wayland, J. V. Minkiewicz, and M. E. Abd-Elmageed, *J. Am. Chem. Soc.*, **96**, 2795 (1974).
(3) P. Rothemund and A. R. Menotti, *J. Am. Chem. Soc.*, **70**, 1808 (1948).
(4) W. Scheuermann and K. Nakamoto, *Appl. Spectrosc.*, **32**, 251 and 302 (1978).
(5) D. Tevault and K. Nakamoto, *Inorg. Chem.*, **15**, 1282 (1976).

0002-7863/81/1503-2162$01.25/0